Research Article | Vol. 26, No. 2 | 22 Jan 2018 | OPTICS EXPRESS A124
Optics EXPRESS

Single scattering properties of non-spherical hydrosols modeled by spheroids

LIPI MUKHERJEE,[1] PENG-WANG ZHAI,[1,*] YONGXIANG HU,[2] AND DAVID M. WINKER[2]

[1]*Joint Center for Earth Systems Technology, Department of Physics, University of Maryland Baltimore County, Baltimore, MD 21250, USA*
[2]*MS 475 NASA Langley Research Center, Hampton, VA 23681-2199, USA*
[*]*pwzhai@umbc.edu*

Abstract: The single scattering properties of hydrosols play an important role in the study of ocean optics, ocean color remote sensing, and ocean biogeochemistry research. Measurements show that hydrosols can be of various sizes and shapes, suggesting general non-spherical models should be considered for the study of single scattering properties of hydrosols. In this work, light scattering by non-spherical hydrosols are modeled by randomly oriented spheroids with the Amsterdam discrete dipole approximation (ADDA) code. We have defined two new parameters to quantify the degree of optical non-sphericity (DONS) and investigated the dependence of DONS on refractive index, size, and aspect ratio. For particles with non-unitary aspect ratios, the magnitude of DONS increases as the refractive index and particle size increase. The dependence of the backscattering fraction on the non-sphericity, size, and refractive index of hydrosols is also studied. It is found that the backscattering fraction is larger for smaller particles as well as for particles with higher refractive indices. Absorptive hydrosols generally have a lower backscattering fraction than non-absorptive hydrosols. This study of light scattering by non-spherical hydrosols would lead to better radiative transfer models in ocean waters and new remote sensing techniques of hydrosol compositions.

OCIS codes: (010.4450) Oceanic optics; (010.4458) Oceanic scattering; (010.1030) Absorption; (010.1350) Backscattering.

References and links

1. C. D. Mobley, *Light and water: Radiative Transfer in Natural Waters* (Academic, 1994).
2. H. R. Gordon, O. B. Brown, and M. M. Jacobs, "Computed relationships between the inherent and apparent optical properties of a flat homogeneous ocean," Appl. Opt. **14**(2), 417–427, (1975).
3. H. R. Gordon and W. R. McCluney, "Estimation of the depth of sunlight penetration in the sea for remote sensing," Appl. Opt. **14**(2), 413–416 (1975).
4. A. Morel and L. Prieur, "Analysis of variations in ocean color," Limnology and Oceanography **22**(4), 709–722 (1977).
5. H. R. Gordon, O. B. Brown, R. H. Evans, J. W. Brown, R. C. Smith, K. S. Baker, and D. K. Clark, "A semianalytic radiance model of ocean color," Journal of Geophysical Research: Atmospheres **93**(D9), 10909–10924 (1988).
6. H. R. Gordon and O. B. Brown, "A theoretical model of light scattering by sargasso sea particulates," Limnology and Oceanography **17**(6), 826–832 (1972).
7. O. B. Brown and H. R. Gordon, "Two component mie scattering models of sargasso sea particles," Appl. Opt. **12**(10), 2461–2465 (1973).
8. M. Jonasz and H. Prandke, "Comparison of measured and computed light scattering in the baltic," Tellus B: Chemical and Physical Meteorology **38**(2), 144–157 (1986).
9. H. R. Gordon, "Mie-theory models of light scattering by ocean," Suspended Solids in Water **4**(73), (2013).
10. H. C. Hulst, *Light Scattering by Small Particles* (Dover, 1981).
11. C. F. Bohren and D. R. Huffman, *Absorption and Scattering of Light by Small Particles* (Wiley-VCH, 1998).
12. T. J. Petzold, "Volume scattering functions for selected ocean waters," Scripps Institution of Oceanography La Jolla Ca Visibility Lab, (1972).
13. K. J. Voss and E. S. Fry, "Measurement of the mueller matrix for ocean water," Appl. Opt. **23**(23), 4427–4439 (1984).
14. E. S. Fry and K. J. Voss, "Measurement of the mueller matrix for phytoplankton," Limnology and Oceanography **30**(6), 1322–1326 (1985).

#307631 https://doi.org/10.1364/OE.26.00A124
Journal © 2018 Received 21 Sep 2017; revised 1 Dec 2017; accepted 12 Dec 2017; published 3 Jan 2018

15. M. Jonasz, "Nonsphericity of suspended marine particles and its influence on light scattering," Limnology and Oceanography **32**(5), 1059–1065 (1987).
16. M. S. Quinby-Hunt, A. J. Hunt, K. Lofftus, and D. Shapiro, "Polarized-light scattering studies of marine chlorella," Limnology and Oceanography **34**(8), 1587–1600 (1989).
17. C. F. Bohren and S. B. Singham, "Backscattering by nonspherical particles: A review of methods and suggested new approaches," Journal of Geophysical Research: Atmospheres **96**(D3), 5269–5277 (1991).
18. D. Stramski and J. Piskozub, "Estimation of scattering error in spectrophotometric measurements of light absorption by aquatic particles from three-dimensional radiative transfer simulations," Appl. Opt. **42**(18), 3634–3646 (2003).
19. A. Quirantes and S. Bernard, "Light scattering by marine algae: two-layer spherical and nonspherical models," J. Quant. Spectrosc. Radiat. Transfer **89**(1), 311–321 (2004).
20. D. Stramski, E. Boss, D. Bogucki, and K. J. Voss, "The role of seawater constituents in light backscattering in the ocean," Progress in Oceanography **61**(1), 27–56 (2004).
21. W. J. Clavano, E. S. Boss and L. Karp-Boss, "Inherent optical properties of non-spherical marine-like particles -from theory to observation," Oceanogr. Mar. Biol. **45**, 11-38 (2007).
22. H. Volten, J. F. de Haan, J. W. Hovenier, R. Schreurs, W. Vassen, A. G. Dekker, H. J. Hoogenboom, F. Charlton, and R. Wouts, "Laboratory measurements of angular distributions of light scattered by phytoplankton and silt," Limnology and Oceanography **43**(6), 1180–1197 (1998).
23. R. D. Vaillancourt, C. W. Brown, R. R. L. Guillard, and W. M. Balch, "Light backscattering properties of marine phytoplankton: relationships to cell size, chemical composition and taxonomy," Journal of Plankton Research **26**(2), 191–212 (2004).
24. B. Sun, G. W. Kattawar, P. Yang, M. S. Twardowski, and J. M. Ivan, "Simulation of the scattering properties of a chain-forming triangular prism oceanic diatom," J. Quant. Spectrosc. Radiat. Transfer **178**, 390–399 (2016).
25. G. Xu, B. Sun, S. D. Brooks, P. Yang, G. W. Kattawar, and X. Zhang, "Modeling the inherent optical properties of aquatic particles using an irregular hexahedral ensemble," J. Quant. Spectrosc. Radiat. Transfer **191**, 30–39 (2017)
26. R. N. Gibson, R. J. A. Atkinson, and J. D. M. Gordon, *Oceanography and Marine Biology: An Annual Review*, 6, Volume 45 (CRC Press, 2007).
27. J. C. Kitchen and J. R. V. Zaneveld, "A three-layered sphere model of the optical properties of phytoplankton," Limnology and Oceanography **37**(8), 1680–1690 (1992).
28. R. J. Olson, E. R. Zettler, and O. K. Anderson, "Discrimination of eukaryotic phytoplankton cell types from light scatter and autofluorescence properties measured by flow cytometry," Cytometry Part A **10**(5), 636–643 (1989).
29. A. J Hunt, M. S Quinby-Hunt, and D. B Shapiro, "Effects of wavelength-dependent absorption on the polarization of light scattered from marine chlorella," Proc. SPIE **1302**, 269-280 (1990).
30. R. W. Schaefer, "Calculations of the light scattered by randomly oriented ensembles of spheroids of size comparable to the wavelength," Ph.D. Thesis State Univ. of New York, Albany (1980).
31. S. Asano and M. Sato, "Light scattering by randomly oriented spheroidal particles," Appl. Opt. **19**(6), 962–974 (1980).
32. P. E. Geller, T. G. Tsuei, and P. W. Barber, "Information content of the scattering matrix for spheroidal particles," Appl. Opt. **24**(15), 2391–2396 (1985).
33. M. Hofer and O. Glatter, "Mueller matrix calculations for randomly oriented rotationally symmetric objects with low contrast," Appl. Opt. **28**(12), 2389–2400 (1989).
34. M. I. Mishchenko, "Light scattering by size–shape distributions of randomly oriented axially symmetric particles of a size comparable to a wavelength," Appl. Opt. **32**(24), 4652–4666 (1993).
35. M. I. Mishchenko and L. D. Travis, "Light scattering by polydispersions of randomly oriented spheroids with sizes comparable to wavelengths of observation," Appl. Opt. **33**(30), 7206–7225 (1994).
36. M. I. Mishchenko, L. D. Travis, and D. W. Mackowski, "T-matrix computations of light scattering by nonspherical particles: a review," J. Quant. Spectrosc. Radiat. Transfer **55**(5), 535–575 (1996).
37. S. Chandrasekhar, *Radiative Transfer* (Dover Publications, 1960).
38. J. E. Hansen and L. D. Travis, "Light scattering in planetary atmospheres," Space Science Reviews **16**(4), 527-610 (1974).
39. T. L. Anderson, D. S. Covert, S. F. Marshall, M. L. Laucks, R. J. Charlson, A. P. Waggoner, J. A. Ogren, R. Caldow, R. L. Holm, F. R. Quant, G. J. Sem, A. Wiedensohler, N. A. Ahlquist, and T. S. Bates, "Performance Characteristics of a High-Sensitivity, Three-wavelength, Total Scatter/Backscatter Nephelometer," Journal Of Atmospheric and Oceanic Technology **13**(5), 967–986 (1996).
40. T. Müller, M. Laborde, G. Kassell, and A. Wiedensohler, "Design and performance of a three-wavelength led-based total scatter and backscatter integrating nephelometer," Atmospheric Measurement Techniques **4**(6), 1291–1303 (2011).
41. M. E. Lee and M. R. Lewis, "A new method for the measurement of the optical volume scattering function in the upper ocean," Journal of Atmospheric & Oceanic Technology **20**(4), 563–571 (2003).
42. M. Twardowski, X. D. Zhang, S. Vagle, J. Sullivan, S. Freeman, H. Czerski, Y. You, L. Bi, and G. Kattawar, "The optical volume scattering function in a surf zone inverted to derive sediment and bubble particle subpopulations," Journal of Geophysical Research: Oceans **117**(C7), 2012 (2012).
43. M. S. Twardowski, E. Boss, J. B. Macdonald, W. S. Pegau, A. H. Barnard, and J. R. V. Zaneveld, "A model for estimating bulk refractive index from the optical backscattering ratio and the implications for understanding particle

composition in case i and case ii waters," Journal of Geophysical Research: Oceans **106**(C7), 14129–14142 (2001).
44. E. Boss, W. S. Pegau, M. Lee, M. Twardowski, E. Shybanov, G. Korotaev, and F. Baratange, "Particulate backscattering ratio at leo 15 and its use to study particle composition and distribution," Journal of Geophysical Research **109**(C1), 2004 (2004).
45. J. M. Sullivan, M. S. Twardowski, P. L. Donaghay, and S. A. Freeman, "Use of optical scattering to discriminate particle types in coastal waters," Appl. Opt. **44**(9), 1667–1680 (2005).
46. J. R. Bottiger, E. S. Fry, and R. C. Thompson, "Phase Matrix Measurements for Electromagnetic Scattering by Sphere Aggregates," in *Light Scattering by Irregularly Shaped Particles* (Springer, 1980), pp. 83–290.
47. Hu, Y., D. Winker, M. Vaughan, B. Lin, A. Omar, C. Trepte, D. Flittner, P. Yang, S. L. Nasiri, B. Baum, R. Holz, W. Sun, Z. Liu, Z. Wang, S. Young, K. Stamnes, J. Huang, and R. Kuehn, "CALIPSO/CALIOP Cloud Phase Discrimination Algorithm," Journal of Atmospheric and Oceanic Technology **26**(11), 2293–2309 (2009).
48. O. Ulloa, S. Sathyendranath, and T. Platt, "Effect of the particle-size distribution on the backscattering ratio in seawater," Appl. Opt. **33**(30), 7070–7077 (1994).
49. D. Stramski and D. A. Kiefer, "Light scattering by microorganisms in the open ocean," Progress in Oceanography**28**(4), 343–383 (1991).
50. S. B. Woźniak and D. Stramski, "Modeling the optical properties of mineral particles suspended in seawater and their influence on ocean reflectance and chlorophyll estimation from remote sensing algorithms," Appl. Opt. **43**(17), 3489–3503 (2004).
51. P. C. Waterman, "Matrix formulation of electromagnetic scattering," Proc. IEEE **53**(8), 805–812 (1965).
52. P. C. Waterman, "Symmetry, unitarity, and geometry in electromagnetic scattering," Phys. Rev. D **3**(4), 825–839 (1971).
53. M. I. Mishchenko, L. D. Travis, and A. A. Lacis, *Scattering, Absorption, and Emission of Light by Small Particles* (Cambridge University Press, 2002).
54. B. R. Johnson, "Invariant imbedding t matrix approach to electromagnetic scattering," Appl. Opt. **27**(23), 4861–4873 (1988).
55. L. Bi, P. Yang, G. W. Kattawar, and M. I. Mishchenko, "Efficient implementation of the invariant imbedding t-matrix method and the separation of variables method applied to large nonspherical inhomogeneous particles," J. Quant. Spectrosc. Radiat. Transfer **116**, 169 – 183, (2013).
56. A. M. Sánchez, E. Zafra, and J. Piera, "Hyperspectral characterization of marine particles based on mie-lorentz and t-matrix codes and a genetic algorithm," 6th Workshop on Hyperstectral Image and Signal Processing: Evolution in Remote Sensing (2014).
57. A. M. Sánchez and J. Piera, "Methods to retrieve the complex refractive index of aquatic suspended particles: going beyond simple shapes," Biogeosciences **13**(14), 4081–4098 (2016).
58. K. Yee, "Numerical solution of initial boundary value problems involving maxwell's equations in isotropic media," IEEE Transactions on Antennas and Propagation **14**(3), 302–307 (1966).
59. P. Yang and K. N. Liou, "Finite-difference time domain method for light scattering by small ice crystals in three-dimensional space," J. Opt. Soc. Am. A **13**(10), 2072–2085 (1996).
60. Q. H. Liu, "The pstd algorithm: A time-domain method requiring only two cells per wavelength," Microwave and optical technology letters **15**(3), 158–165 (1997).
61. T. W. Lee and S. C. Hagness, "Pseudospectral time-domain methods for modeling optical wave propagation in second-order nonlinear materials," J. Opt. Soc. Am. B **21**(2), 330–342 (2004).
62. E. M. Purcell and C. R. Pennypacker, "Scattering and absorption of light by nonspherical dielectric grains," The Astrophysical Journal **186**, 705–714 (1973).
63. B. T. Draine, "The discrete-dipole approximation and its application to interstellar graphite grains," The Astrophysical Journal **333**, 848–872 (1988).
64. M. A. Yurkin and A.G. Hoekstra, "The discrete dipole approximation: An overview and recent developments," J. Quant. Spectrosc. Radiat. Transfer **106**(1-3), 558–589 (2007).
65. P. Yang and K. N. Liou, "Geometric-optics–integral-equation method for light scattering by nonspherical ice crystals," Appl. Opt. **35**(33), 6568–6584 (1996).
66. P. Yang and K. N. Liou, "Light scattering by hexagonal ice crystals: solutions by a ray-by-ray integration algorithm," J. Opt. Soc. Am. A **14**(9), 2278–2289 (1997).
67. L. Bi, P. Yang, G. W. Kattawar, Y. Hu, and B. A. Baum, "Scattering and absorption of light by ice particles: Solution by a new physical-geometric optics hybrid method," J. Quant. Spectrosc. Radiat. Transfer **112**(9), 1492 – 1508, (2011).
68. M. A. Yurkin, A. G. Hoekstra, R. S. Brock, and J. Q. Lu, "Systematic comparison of the discrete dipole approximation and the finite difference time domain method for large dielectric scatterers," Opt. Express **15**(26), 17902–17911 (2007).
69. M. A. Yurkin, V. P. Maltsev, and A. G. Hoekstra, "The discrete dipole approximation for simulation of light scattering by particles much larger than the wavelength," J. Quant. Spectrosc. Radiat. Transfer **106**(1), 546–557 (2007).
70. M. Nicolet, M. Schnaiter, and O. Stetzer, "Circular depolarization ratios of single water droplets and finite ice circular cylinders: a modeling study," Atmospheric Chemistry and Physics **12**(9), 4207–4214 (2012).

Optics EXPRESS

1. Introduction

Ocean optics quantitatively studies single or multiple scattering of electromagnetic waves in ocean waters, which is essential for understanding many important processes, such as, underwater navigation, ocean primary production through photosynthesis, and environmental remote sensing [1]. The spatial, angular, and spectral distributions of underwater light field depends upon the absorption and scattering characteristics, the so-called inherent optical properties (IOPs), of oceanic particles or hydrosols [1]. Particles responsible for scattering and absorption of light in ocean include phytoplankton, non-algal particles of both organic and inorganic origin, and many other particle types [1]. These particles have different IOPs due to different microphysical properties such as particle size distribution, shape, and dielectric properties. The modeling of single scattering properties of hydrosols with different microphysical parameters is the basis of radiative transfer in ocean and is critical in interpreting the ocean radiation field measured by in situ or remote sensing sensors [2–5]. Understanding the IOPs of hydrosols leads to better radiative transfer models in ocean waters and new remote sensing techniques of hydrosol compositions.

Traditionally, hydrosols have been modeled as spherical particles [6–9] due to the fact that the Mie theory provides a reasonable and low-computational-cost approximation for the IOPs of hydrosols [10,11]. However, scanning electron microscope (SEM) images and other measurements show that hydrosols can be of various sizes and shapes which suggests that general non-spherical models should be considered for the study of IOPs of hydrosols [12–30]. Studies have shown that the spherical model is inadequate in predicting a number of light scattering properties, including the projected areas for non-spherical marine particles [15], Mueller matrix elements for Chlorella culture [16], backscattering coefficients for irregular shaped particles [17, 19], and volume scattering function [27].

Non-spherical numerical models are particularly important for simulating the backscattering properties of hydrosols. Stramski and Piskozub [18] found the backscattering ratios of two species of phytoplankton to be three to ten times larger than those predicted by the Mie theory. Quirantes and Bernard [19] studied heterogeneous spheres and concluded that backscattering efficiency is sensitive to shape of the particle. The modeling of phytoplankton and bacteria as homogeneous spheres results in underestimated backscattering coefficient values which was called by Stramski et al. [20] in 2004 as the 'missing backscattering enigma'. Moreover, Volten et al. [22] and Vaillancourt et al. [23] shows that lab measurements of the backscattering coefficient of hydrosols do not agree with the theoretical values based on homogeneous spheres. Recently, Xu et al. [25] highlight the non-spherical effects on backscattering of aquatic particles particularly the backscattering ratios, backscattering volume scattering functions and degree of linear polarization for both organic and inorganic particles.

To date the concept of non-sphericity has been used in the literature [30–36], but without a clear definition. In this study, we introduce two parameters to formally define the degree of optical non-sphericity (DONS), which can be used to quantify the magnitude of non-sphericity in terms of scattering properties. Specifically, DONS can be represented as an integral of $1 - P_{22}/P_{11}$ (or $(P_{44} - P_{33})/P_{11}$) over the whole range of the scattering angles, where P_{11}, P_{22}, P_{33}, and P_{44} are Mueller scattering matrix elements (see eqs. (1) to (5) for definitions). For spherical particles, DONS is zero, whereas, for non-spherical particles, DONS would vary depending on the particle size, index of refraction, and geometric shape. The linear backscattering depolarization ratio (δ) can also be used to quantify the particle's non-sphericity because of its sensitivity to nonsphericity [11, 30–38]. In this paper DONS is computed and analyzed for spheroidal shaped hydrosols with different aspect ratios of both organic and inorganic origin. The results show substantial variation of DONS for hydrosols with different characteristics and composition which is important for future studies of hydrosols. Such information about DONS and depolarization by the scatterers will lead to better identification of particles based on their scattering properties.

In this paper, backscattering fraction is also studied and its sensitivity to particle size, non-

sphericity and refractive indices is explored. It can be directly measured by commercial integrating nephelometers [39, 40]. It can also be obtained by measuring the underwater volume scattering function [41, 42]. The backscattering fraction is important in interpreting the remote sensing reflectance data [2–5], which can provide information about the particle's refractive index as shown by Twardowski et. al in 2001 [43] and Boss et. al in 2004 [44]. The sensitivity of this quantity towards particle's refractive index, size, and shape, makes it important for particle identification as shown by Sullivan et al. in 2005 [45].

This paper is organized as follows: Sec. 2 describes the definitions used in this work; Sec. 3 shows the result of this study; Sec. 4 summarizes the conclusion reached in this study.

2. Theory

The intensity and polarization features of the scattered light from a particle can be completely described by a 4×4 matrix called the scattering or Mueller matrix. The scattering matrix for a randomly oriented particle with a plane of symmetry has only six independent non-zero elements and can be written as [10, 11]:

$$\begin{bmatrix} I_s \\ Q_s \\ U_s \\ V_s \end{bmatrix} = \frac{\overline{C_{sca}}}{4\pi r^2} \begin{bmatrix} P_{11}(\theta) & P_{12}(\theta) & 0 & 0 \\ P_{12}(\theta) & P_{22}(\theta) & 0 & 0 \\ 0 & 0 & P_{33}(\theta) & P_{34}(\theta) \\ 0 & 0 & -P_{34}(\theta) & P_{44}(\theta) \end{bmatrix} \begin{bmatrix} I_i \\ Q_i \\ U_i \\ V_i \end{bmatrix}, \tag{1}$$

where I, Q, U, V are the Stokes parameters; the subscripts i and s denote the incident and scattered light, respectively; $\overline{C_{sca}}$ is the scattering cross-section averaged over all orientations and r is the distance from the scatterer to the observer and θ is the scattering angle. The $P_{11}(\theta)$ element, known as the phase function, satisfies the normalization condition

$$\frac{1}{2}\int_0^\pi P_{11}(\theta)\sin\theta d\theta = 1. \tag{2}$$

The reduced Mueller matrix elements are those divided by P_{11} such as P_{22}/P_{11}, P_{33}/P_{11}, P_{44}/P_{11} and P_{12}/P_{11}, which are used to separate the intensity dependent effects from the polarization effects.

One primary focus of this paper is to formally define the non-sphericity of hydrosols and explore its sensitivity to size parameter, shape, and refractive index. The nonsphericity can be studied in terms of three parameters. The first parameter is linear backscattering depolarization ratio δ:

$$\delta = \frac{P_{11}(\pi) - P_{22}(\pi)}{P_{11}(\pi) + P_{22}(\pi)}, \tag{3}$$

which is zero/nonzero for spherical/nonspherical particles [11, 37, 38, 46]. This element is studied because of its importance in lidar remote sensing [47]. The other two parameters are defined as:

$$\epsilon = \int_0^\pi \left(1 - \frac{P_{22}(\theta)}{P_{11}(\theta)}\right)\sin\theta d\theta, \tag{4}$$

$$\chi = \int_0^\pi \left(\frac{P_{44}(\theta) - P_{33}(\theta)}{P_{11}(\theta)}\right)\sin\theta d\theta, \tag{5}$$

which take into account the contribution of non-spherical characteristics of hydrosols at all scattering angles.

Backscattering fraction is another important quantity which helps in characterizing the optical properties of hydrosols. It is defined as:

$$B = \frac{\int_{\pi/2}^\pi P_{11}(\theta)\sin\theta d\theta}{\int_0^\pi P_{11}(\theta)\sin\theta d\theta}, \tag{6}$$

Optics EXPRESS

the ratio of light energy scattered in the backward direction to the total scattered light energy [1].

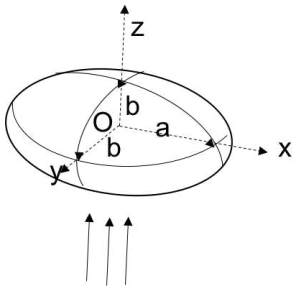

Fig. 1. The spheroid is centered at origin O with semi-axes a and b aligned along coordinate axes and x is the symmetry axis. The light is incident along the z-axis.

In this paper, the single scattering properties of randomly oriented spheroidal shaped hydrosols are studied. Figure 1 shows the spheroid model used in the study, where a and b are the major and minor semi-axes respectively. The ratio b/a is the aspect ratio which ranges from 0.5 to 1.5 in this work. The real indices of refraction used are 1.02, 1.05, and 1.11. Both absorptive and non-absorptive hydrosols are studied. For absorptive hydrosols, the imaginary part of the refractive index (m_i) is 0.01, which is based on the work done by Osvaldo et al. [48] who showed that even strongly absorbing phytoplankton have m_i values less than or equal to 0.01. Organic matter like phytoplankton, bacteria, detritus, and viruses have low refractive indices (close to unity) whereas inorganic particulates like minerals (range from unity to 1.2 relative to water) and oil (around 1.10 relative to water) are associated with high refractive indices [49, 50]. Studying particles with aforementioned refractive indices would not only help in differentiating inorganic and organic oceanic particles but also in better modeling of apparent optical properties of ocean waters.

There are a number of exact numerical methods available to study light scattering by non-spherical particles. The T-matrix method can be used to study rotationally symmetric particles [24, 51–57]. The scattering properties of particles with arbitrary geometry can be studied using the more flexible numerical methods, including the Finite Difference Time Domain (FDTD) [58, 59], the pseudo spectral time domain (PSTD) [60, 61], and the discrete dipole approximation (DDA) [62–64]. For scatterers with large size parameter, geometric methods [65–67] can be used. We used the Amsterdam Discrete Dipole Approximation code (ADDA) [64, 68], which is a C software package based on discrete dipole approximation method. The ADDA code is robust, efficient for particles with low refractive indices (smaller than 1.4), and applicable to particles of arbitrary shape and composition [68]. Its capability to parallelize single orientation simulations makes it suitable for particles with size parameter as high as 160 with refractive index m=1.05 [69]. In this work, the maximum value of the volume equivalent size parameter x is about 83 and the volume equivalent size parameter is defined in terms of the radius of volume equivalent spheres r:

$$x = \frac{2\pi r}{\lambda}, \tag{7}$$

where λ is wavelength.

Optics EXPRESS

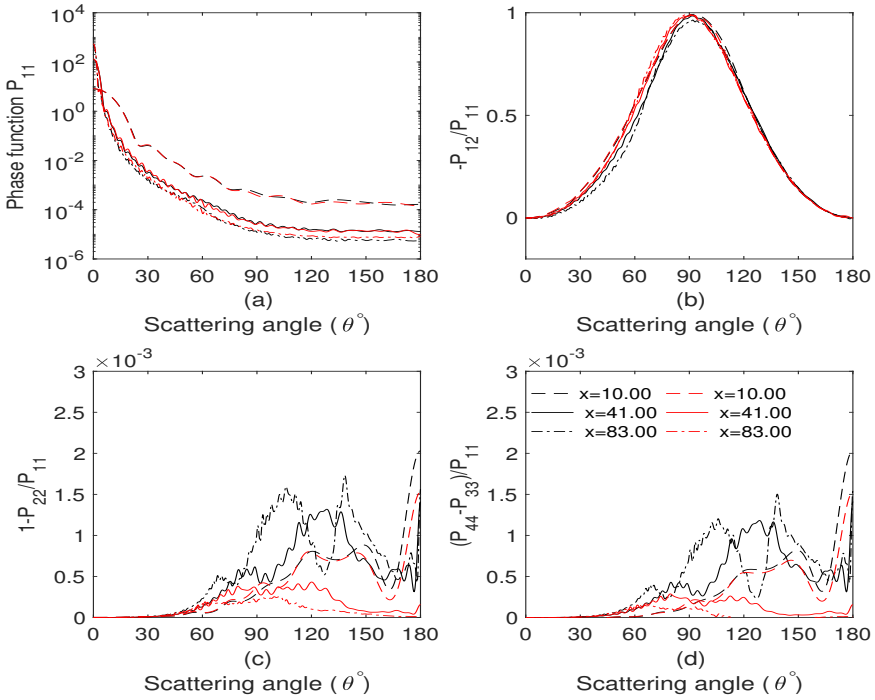

Fig. 2. The phase function P_{11} and reduced Mueller matrix elements $-P_{12}/P_{11}$, $1-P_{22}/P_{11}$, and $(P_{44}-P_{33})/P_{11}$ of spheroidal shaped hydrosols with the refractive index m=1.02 and the aspect ratio of 1.5. The legend in Fig. 2(d) applies to all four subplots in Fig. 2. The red lines represent absorptive cases, while the black lines represent non-absorptive cases. This color code applies to all other figures.

3. Results and discussion

3.1. Mueller matrix

Figures 2 and 3 show the Mueller matrix elements of hydrosols for different volume equivalent sizes with the aspect ratio of b/a=1.5. The refractive indices are m=1.02 and 1.11, with both nonabsorptive (imaginary refractive index of m_i=0) and absorptive (mi=0.01) cases are included. For particles with the same size, hydrosols with lower refractive index (Fig. 2a)) have lower backscattering when compared to hydrosols with higher refractive index (Fig. 3a)). For hydrosols with low refractive indices it is difficult to distinguish between absorptive and non-absorptive hydrosols by phase function P_{11} and degree of linear polarization $-P_{12}/P_{11}$, which is however easier to do in terms of $1-P_{22}/P_{11}$ and $(P_{44}-P_{33})/P_{11}$. We notice that although the particles are non-spherical in shape, for small refractive indices, the $-P_{12}/P_{11}$ element behaves similar to spherical particles with maximum polarization at 90° as shown in Fig. 2(b). On the other hand, the depolarization ratio $1-P_{22}/P_{11}$ and $(P_{44}-P_{33})/P_{11}$ (which are zero for spherical particles) are non-zero near backscattering region for both high and low refractive indices hydrosols. The side scattering feature observed in $1-P_{22}/P_{11}$ and $(P_{44}-P_{33})/P_{11}$ can aid in distinguishing particles with aspect ratios other than unity. The aforementioned characteristics are observed both for non-absorptive hydrosols (black) and absorptive hydrosols (red) in Figs. 2 and 3.

Optics EXPRESS

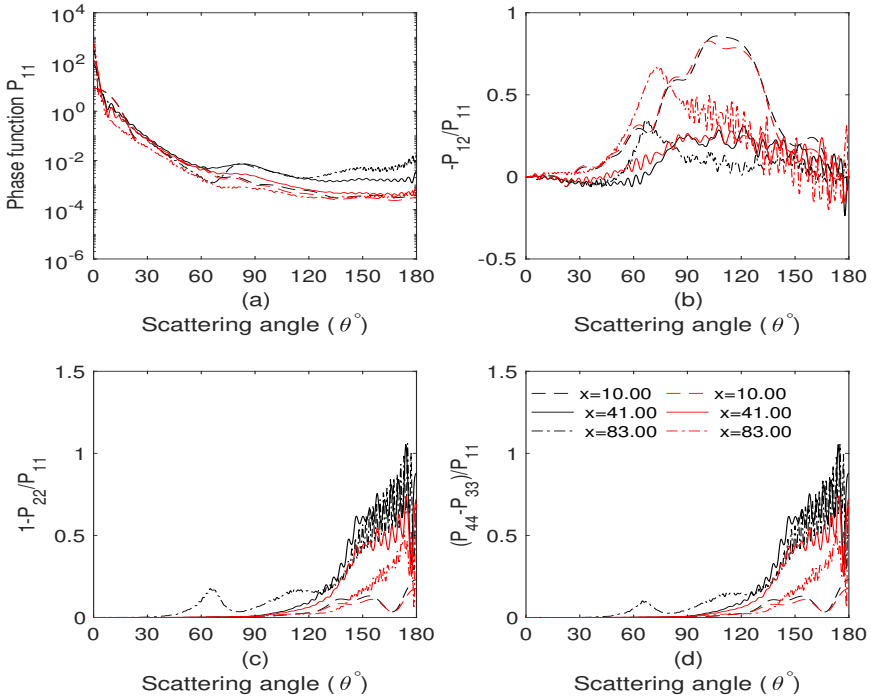

Fig. 3. The same as Fig. 2 except for the refractive index m=1.11

3.2. *Optical non-sphericity of hydrosols*

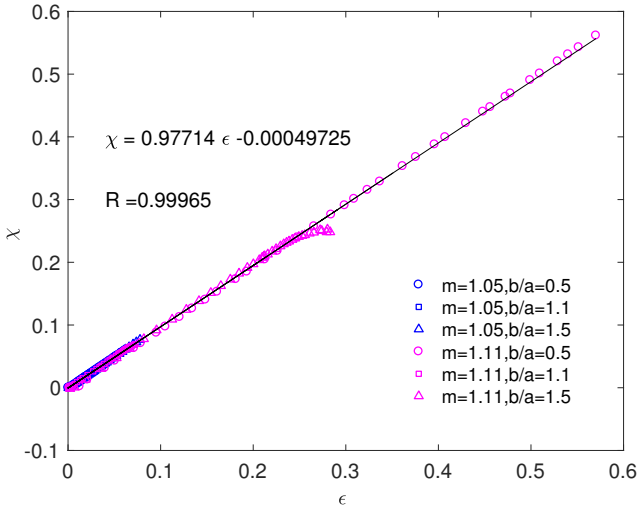

Fig. 4. Relationship between χ and ϵ.

It is instructive to investigate the relationship between the three representations of degree of

optical non-sphericity. Figure 4 shows that χ and ϵ are linearly related (correlation coefficient R>0.99) for non-absorptive hydrosols. The same linear relationship exists for absorptive hydrosols (not shown). Both χ and ϵ have higher values for particles with the aspect ratio of 0.5 when compared to particles with the aspect ratio of 1.5 for m=1.11. This is consistent with Hofer et al. [33], where the reduced elements P_{22}/P_{11}, P_{33}/P_{11}, and P_{44}/P_{11} were higher for aspect ratios less than unity. This is further demonstrated in Fig. 5 which shows the dependence of DONS (ϵ) on the volume equivalent size parameter (x). The two quantities χ and ϵ show a linear dependence on each other. Therefore we will use ϵ to represent degree of optical non-sphericity in the remainder of this paper.

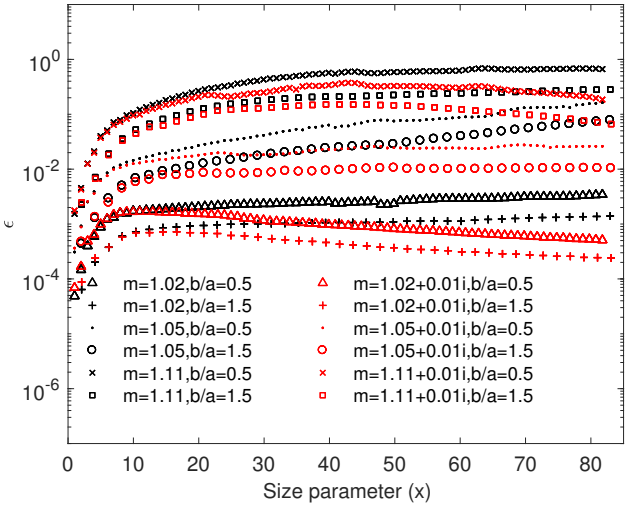

Fig. 5. DONS (ϵ) as a function of with the volume equivalent size parameter.

Figure 5 shows that the DONS value is low for small particles and becomes larger as particle size increases until an asymptotic region is reached. Particles with small size parameter or low refractive index fall into the Rayleigh-Gans [11] scattering limit, and thus behave similarly to spherical particles, with low values of DONS. It is further observed that, as the size increases, the DONS variation with respect to refractive indices becomes more pronounced. DONS is less for hydrosols with an aspect ratio of 1.5 when compared to hydrosols with an aspect ratio of 0.5 for the same refractive index. For a constant aspect ratio, DONS increases with an increase of refractive index of hydrosols. In general, compared to non-absorptive hydrosols, absorptive hydrosols have a lower DONS.

Figure 6 shows the linear backscattering depolarization ratio (δ) as a function of the volume equivalent size parameter (x). Particles with small size or low refractive index are in the Rayleigh-Gans [11] scattering regime, which have low δ values similar to spherical particles [31, 70]. For particles with higher refractive index, as the size increases, δ approaches an asymptotic value. We notice that higher depolarization values are associated with aspect ratios deviating farther from one. In general, compared to non-absorptive hydrosols, absorptive hydrosols have a lower δ.

Figure 7 shows the relationship between the linear backscattering depolarization ratio δ and DONS (ϵ). For the case of b/a=1.1, the depolarization ratio δ is much larger than ϵ. As the aspect ratio deviates far from unity, ϵ and δ are showing different sensitivity to particle size, which can be used to differentiate hydrosols with different aspect ratios.

Optics EXPRESS

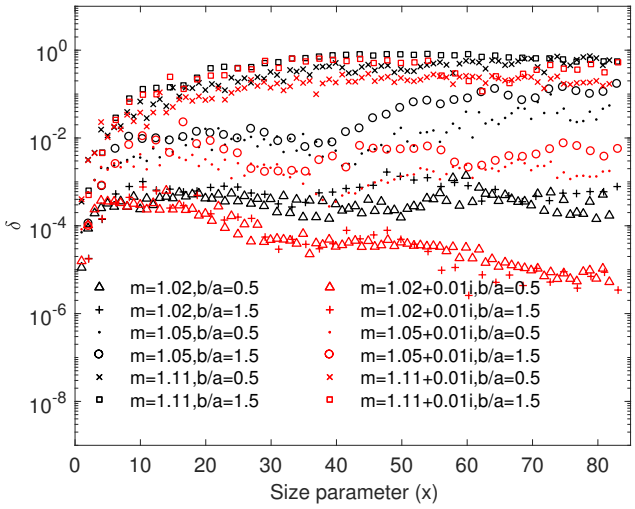

Fig. 6. The depolarization ratio δ as a function of the volume equivalent size parameter.

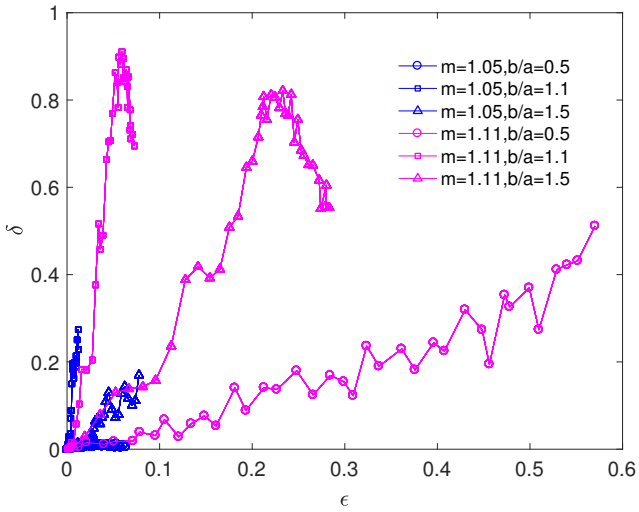

Fig. 7. Relationship between δ and ϵ.

3.3. *Backscattering fraction*

Figure 8 shows the dependence of backscattering fraction on the volume equivalent size parameter (x). The backscattering fraction is higher for small particles due to reduced diffraction. It can be observed that backscattering fraction is almost independent of refractive index for small particles (both for absorptive and non-absorptive). For larger particles, the backscattering fraction is larger for larger refractive indices, which is consistent with the phase function shown in Figs. 2a and 3a. Osvaldo et al. have similar findings regarding the backscattering fraction [48]. In addition, absorptive hydrosols reduce the backscattering fraction. We also notice that absorptive and non-absorptive hydrosols at low refractive index have almost equal backscattering fraction. Last

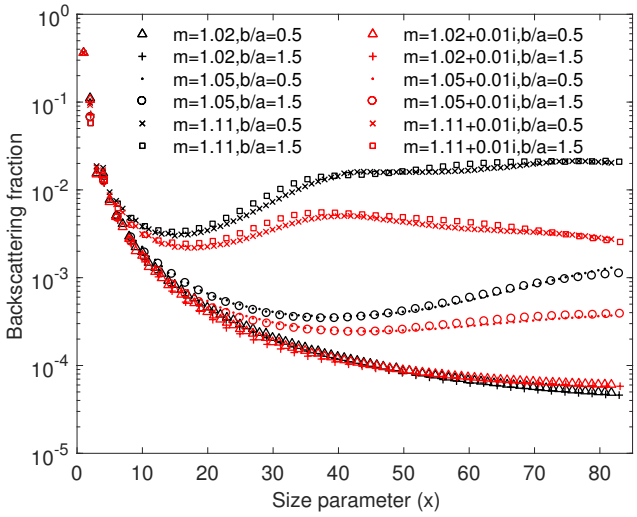

Fig. 8. Backscattering fraction as a function of the volume equivalent size parameter.

but not least, the backscattering fraction is almost independent on the aspect ratio, as long as the volume equivalent size parameter is the same.

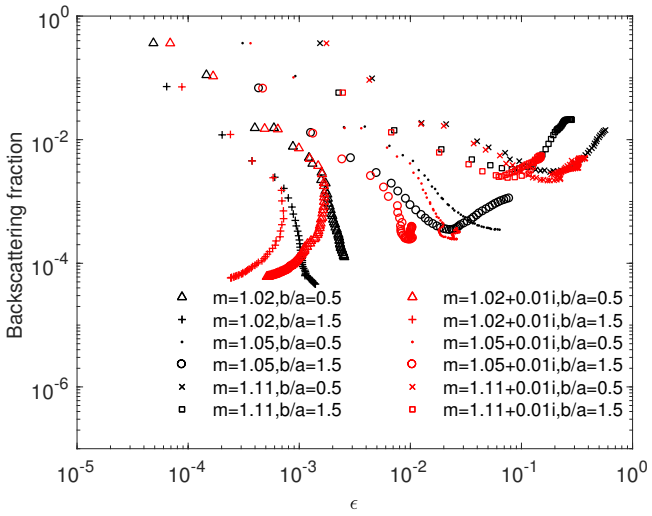

Fig. 9. Backscattering fraction versus DONS (ϵ).

Figure 9 shows the backscattering fraction versus DONS (ϵ). Here both the backscattering fraction and DONS are high for particles with higher refractive indices. In general, compared to non-absorptive hydrosols, absorptive hydrosols have lower backscattering fraction and DONS. Both aspect ratio and refractive index have pronounced impacts on backscattering fraction and DONS. This is evident from the lines with different refractive indices and aspect ratios being clearly separated.

Optics EXPRESS

4. Conclusion

It has been found from measurements that hydrosols present in both open ocean and coastal areas are generally non-spherical in shape. Thus, the knowledge of inherent optical properties of non-spherical hydrosols is vital to accurately model the light propagation in different kinds of water. In this paper we formally define the degree of optical non-sphericity (DONS) in terms of two parameters ϵ and χ, which are combined with the linear depolarization ratio δ to explore the dependence of optical nonsphericity on particle size, aspect ratio, and refractive index for spheroidal hydrosols. It is found that ϵ and χ are highly linearly correlated and hence, either of them can be used to represent DONS. Our simulation shows that DONS is larger for particles with higher refractive indices, larger sizes, or larger deviation from unitary aspect ratio. For refractive indices close to 1, particles fall into the Rayleigh-Gans scattering region where ϵ is only weakly dependent on size. For a larger refractive index, ϵ increases with particle size until it reaches an asymptotic region where little variation of DONS is observed. The linear depolarization ratio shows similar patterns as ϵ, but has different sensitivity to aspect ratio. The backscattering fraction was also studied in this work because of its innumerable applications in identifying the characteristics of hydrosols. It is found that the backscattering fraction is larger for smaller particles as well as for particles with higher refractive indices. Absorptive hydrosols generally have lower backscattering fraction than non-absorptive hydrosols. The optical properties of non-spherical hydrosols and their interdependence on size, refractive index, and aspect ratio can lead to better differentiation of particles with different morphologies and better radiative transfer modeling for ocean waters.

Funding

NASA (NNX15AB94G, NNX15AL87G, 80NSSC17K0366).

Acknowledgments

This work was supported by NASA grant NNX15AB94G from the Atmospheric Composition research programs; and NASA grant NNX15AL87G from the OCO2 science team. The authors also thank Science System Applications Inc. for contractual support. This work was also supported by NASA Headquarters under the NASA Earth and Space Science Fellowship Program - Grant 80NSSC17K0366.

The hardware used in the computational studies is part of the UMBC High Performance Computing Facility (HPCF). The facility is supported by the U.S. National Science Foundation through the MRI program (grant nos. CNS-0821258 and CNS-1228778) and the SCREMS program (grant no. DMS-0821311), with additional substantial support from the University of Maryland, Baltimore County (UMBC).